11, 206 (1960)].
[9]Y. Koh, O. Miyatake, and Y. Watanabe, Nucl. Phys. 32, 246 (1962).
[10]W. D. Brewer and D. A. Shirley, Phys. Rev. Letters 20, 885 (1968).
[11]We employ units in which $m = c = \hbar = 1$ (m is the electron mass), and $e^2 = \alpha = \frac{1}{137}$. In terms of the standard Dirac matrices $\vec{\alpha}$ and β, the γ matrices are defined as $\vec{\gamma} = -i\beta\vec{\alpha}$, $\gamma_4 = \beta$, $\gamma_5 = \gamma_1\gamma_2\gamma_3\gamma_4$. Also, $\vec{\Sigma} = -\gamma_5\vec{\alpha}$ and the Pauli adjoint is defined by $\bar{\phi} = \phi^+\gamma_4$. Our normalization volume is denoted by V.
[12]In the nuclear wave functions, the coordinates of all the nucleons except the one undergoing the capture process have been suppressed. It is to be understood that an integration over this coordinate implies an integration over the coordinates of the other nucleons as well. A summation over all the protons in the initial nucleus is also implied.
[13]It is assumed that $1s$-state capture is energetically allowed, so that our approximation amounts to including the two most important s-state contributions as well as the two most important p-state contributions. On this basis we neglect the very small contribution from $3s$-state capture. However, should $1s$-state capture be energetically forbidden, inclusion of this latter contribution would then be in order.
[14]See Glauber and Martin, Ref. 4, Sec. 9.
[15]W. D. Brewer, University of California Radiation Laboratory Report No. UCRL-19533, 1969 (unpublished).
[16]J. L. Olsen, L. G. Mann, and M. Lindner, Phys. Rev. 106, 985 (1957).
[17]W. D. Brewer, private communication.

PHYSICAL REVIEW C VOLUME 3, NUMBER 1 JANUARY 1971

Proton-Proton Elastic Scattering from 9.6 to 13.6 MeV*

Nelson Jarmie, J. H. Jett, J. L. Detch, Jr.,† and R. L. Hutson
Los Alamos Scientific Laboratory, University of California, Los Alamos, New Mexico 87544
(Received 24 August 1970)

Accurate differential-cross-section data for proton-proton elastic scattering are presented at 9.690, 9.918, and 13.600 MeV. These data agree with current energy-dependent phase-shift analyses and resolve discrepancies between previous sets of data and between those data and the phenomenological analysis.

I. INTRODUCTION

The importance of nucleon-nucleon scattering information to the understanding of the strong nuclear force can hardly be overestimated. Not only is it the most accessible process concerning the strong interaction between simple noncomposite nuclear particles, but it is greatly benefited by the large energy region free from strongly interacting inelastic channels. A detailed theoretical description of the scattering does not now exist, although there has been progress in the one-boson-exchange model.[1] A unique and complete phenomenological description is very desirable as a basis for a theoretical description and for the correlation of experiments, and, to a given accuracy, should eliminate the necessity for performing further experiments in the region of interest. In proton-proton scattering several energy-dependent phase-shift analyses[2,3] that give a good fit to all data up to 400 MeV have been published. Some of the remaining difficulty has been in the region below 10 MeV, where involved electromagnetic corrections[4] are necessary, partly because of the accuracy of the data. There has also been disagreement between sets of experimental data and difficulty in fitting some of the data without serious problems in the phenomenological method.

In particular, near 10 MeV the cross-section data of Johnston and Young[5] (Minnesota) at 9.69 MeV disagree markedly with the data at 9.918 MeV of Slobodrian *et al.*[6] (Berkeley) in both shape and absolute magnitude. Sher, Signell, and Heller[4] show that the central phase parameter, $9\Delta_C = \delta_{10} + 3\delta_{11} + 5\delta_{12}$ where the δ_{LJ}'s are the P-wave phases, extracted from the Berkeley and Minnesota data disagree by several standard deviations. MacGregor, Arndt, and Wright,[7] using an energy-dependent phase-shift analysis, have shown the Berkeley 9.918-MeV data to be inconsistent with the Berkeley data at 6.141 and 8.097 MeV when combined with other data at nearby energies. In addition, Holdeman, Signell, and Sher[8] (HSS) found the $^1S_0$ phase and the Δ_C parameter extracted from the Berkeley data incompatible with a reasonable phenomenological prediction, and that in order to make a fit, serious readjustment of fits to a number of well-accepted data at other energies would be necessary (see Figs. 2 and 3 of Ref. 8).

To help resolve these inconsistencies, we measured accurate differential cross sections at 9.690 and 9.918 MeV. These results were reported in an earlier Letter[9] and analyzed by HSS. They found that the angular shape of our data agreed with their

prediction and with the Minnesota data, but that our absolute values were such that the $^1S_0$ phase from our data was also difficult to fit, in agreement with the Berkeley data.

To help resolve this discrepancy we undertook two courses of action. First, since the $^1S_0$ phase is strongly affected by the absolute values of the data, we planned a thorough examination and recalibration of all experimental parameters that affect the absolute normalization in our previous measurements at 9.690 and 9.918 MeV. We also restudied the assumptions and approximations made in the reduction of the data, especially at small angles. Secondly, we measured an accurate angular distribution at a nearby energy, 13.600 MeV, to help tie down the absolute value and search for possible energy-dependent systematic errors.

With one exception, the recalibrations and remeasurements produced no significant results outside expected errors. We did find a gross systematic error in the device used to measure the width of the slits in the detector; and the value of the G factor and the cross sections are directly affected. The correction increases our 9.690- and 9.918-MeV absolute values about 2%, and brings the absolute values close to the predictions of the multienergy analysis of Sher, Signell, and Heller.[4] The 13.600-MeV data also agree with the phenomenological analysis. In brief, the present work claims to have resolved the inconsistencies in proton-proton scattering in the 10-MeV region. A preliminary report of this later work and a discussion of its significance has been published.[10] The present paper will present the experiment in detail and summarize the final results. An even more detailed account of the apparatus and methods will be found in the thesis of Detch.[11]

II. EXPERIMENTAL EQUIPMENT

A. Scattering Chamber

As shown schematically in Fig. 1, the scattering chamber used was an evacuated 76.2-cm-i.d. cylindrical chamber equipped with digital encoding of the moving components. The detector mount with included collimating system was positioned in a precisely machined groove in the rotating turntable floor of the chamber and aligned by optical telescope relative to the beam direction. Optical tests provided a measure of the chamber turntable eccentricity. The displacement of the turntable axis from the beam line was about 280 μm, and this improper motion was taken into account in the calculation of the G factor and proper angle in the cross-section calculations. Variation of the G factor due to this effect was smaller than 0.4% and the correction to the angle was 0.03°. (See Sec. IV on errors.)

The chamber was electrically isolated from ground, and was in electrical contact with the last beam collimating aperture to allow measurement of this current. Chamber vacuum was provided by a liquid-nitrogen-trapped oil diffusion pump which usually maintained chamber vacuum at 5×10^{-7} Torr.

B. Beam and Beam Optics

Negative hydrogen ions were accelerated by the Los Alamos electrostatic accelerator (one stage) and injected into the tandem Van de Graaff accelerator (two stage). "Three-stage" operation was used to permit the increased beam stability achieved by operating the accelerating heads at relatively low voltages. The proton beam emerged from the accelerator and was momentum-analyzed in a 90° double-focusing bending magnet whose field was stabilized by a nuclear magnetic resonance device, and passed through several small-angle steering magnets, strong-focusing magnetic quadrupole lenses, and appropriate collimators.

The positioning of the various collimating slits and active elements in the beam-optics system was optimized using a computer optics program to obtain a long narrow waist in the beam profile in the vicinity of the gas target to assure a nearly divergence-free beam at the entrance to the target. The phase-space emittance at the gas target was less than 0.13 mrad cm in either plane.

Current monitoring was provided at each collimating aperture in the beam tube and permitted the focusing and steering to be optimized to obtain nearly 100% transmission through the prechamber slits for low background and good definition of the geometry. The final collimating aperture, a rectangle measuring 1.0 mm horizontally by 1.5 mm vertically, was located approximately 2 mm from the target entrance foil and was fabricated from tantalum. Slit parameters were chosen

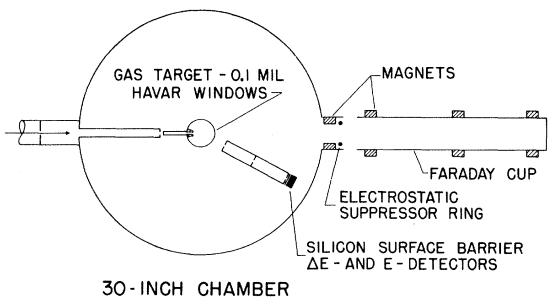

FIG. 1. Simplified drawing of the scattering chamber, final beam-defining apertures, target, Faraday cup, and detector telescope with collimators.

so as to be able to stop 25-MeV protons and to minimize the effect of slit-edge scattering. This aperture and a slightly larger aperture located approximately 1.2 m upstream defined the beam direction with a maximum possible angular uncertainty for a line beam of ±0.13°. However, minor adjustments of either steering or focusing elements showed that the beam very nearly filled both of these apertures, and the maximum deviation from the central direction was less than 0.06°. Wander of the beam during a given left-right run was less than ±0.02°. (See Sec. IV on errors.) In general, it was not possible to adjust any element in the beam-optics system without showing a current on one or both of these two final collimators, and these currents were observed throughout the experiment to assure proper beam-optics characteristics.

C. Target and Gas-Handling System

The gas target was machined from a solid brass cylinder 9.3 cm in diameter to provide a target volume of this diameter and an internal height of about 1.6 cm. The upper and lower brass surfaces were supported in a cantilever manner by a single internal post where the beam enters the target volume, allowing an operating data range of ±168°. This post has a pre-target snout approximately 7.6 cm long which supports the entrance foil and contains an internal scraper slit to suppress angular divergence of the beam caused by multiple scattering in the entrance foil. The target foil was made of Havar,[12] a cobalt "superalloy," and measured about 1.9 cm by 26.7 cm, being 2.3 μm (0.09 mil) thick. The foil was attached to the target body using Armstrong A-6 epoxy, a process guaranteed to occupy several entertaining hours. The target was normally operated at a pressure of 175 Torr. Proton beam currents of as much as 2 μA have been used with this target, with the only failure being the decomposition of the epoxy around the entrance foil caused by inadvertantly allowing 2 μA of 13.6-MeV protons to strike the epoxy.

A gas manifold was attached to the target in such a manner as to allow the entire system to be evacuated at high vacuum and to permit various spectroscopic-grade gasses to be introduced into the target in an easily controllable manner. Stainless-steel needle valves were incorporated, with a minimal amount of organic materials, such as O-rings, in the system because of its occasional use with tritium and to minimize contaminants.

The target body was electrically isolated from the remainder of the system and provided a means for measuring any beam current intercepted by the target.

D. Temperature and Pressure Measurements

Target temperature was measured by the attachment to the target body of a Chromel-Alumel thermocouple which was read and recorded on a Brown chart recorder. This system was frequently calibrated with a precision temperature bath. Temperature information was interfaced to the on-line computer and was read automatically and manually into the data records.

Pressure measurements were provided by an electronic pressure transducer[13] of a diaphram capacitance-bridge type. This instrument was calibrated with a precision fused-quartz pressure gauge accurate to ±0.02 Torr. Long-term drift of the transducer calibration was found to obey a proper linear relation to its reading at zero pressure, and this is included in the pressure correction terms for the given run. The voltage output from this pressure transducer was measured on digital voltmeters, one of which permitted manual recording of the pressure and the other of which was interfaced into the computer to provide automatic pressure recording. As a cross check a Wallace-Tiernan[14] mechanical diaphram-type pressure gauge was included in the system. The mechanical gauge readings were consistent with the transducer's measurements to within its accuracy (0.3 Torr). The accuracy of the pressure transducer was ±0.2 Torr, limited primarily by the reproducibility of the instrument.

E. Detectors and Collimators

Three silicon surface-barrier detectors of approximate thicknesses of 40, 250, and 2000 μm and areas of 100, 150, and 150 mm^2, respectively, were combined into a telescope to provide particle-mass identification and background reduction with coincidence requirements. These detectors were cooled below room temperature by a thermoelectric cooler to reduce noise and improve energy resolution, though the thinness of the first detector prevented cooling below 0°C.

The detector collimating system was composed of an entrance slit located approximately 3 cm from the gas target foil and 8 cm from the target center, and a rear slit system located 30 cm from the target center, with the detector stack immediately behind the rear slits. This collimating system was then enclosed in a shield to prevent stray particles from reaching the detectors. A scraper slit was placed midway between the two defining collimating apertures to prevent scattering from the collimator walls. A small bar magnet was placed midway between the two defining apertures to prevent low-energy electrons from reaching the detectors.

The scattering full width at half maximum (FWHM) angular range seen by the detectors varied from 0.4° at forward angles to 0.7° at backward angles. This angular width includes contributions from foil multiple scattering, the 0.3° acceptance of the detector slits, and the primary-beam divergence. The data analysis program calculated the energy of the detected particles and corrected the detector efficiency to account for nuclear reactions occurring in the silicon detectors.[15] The largest correction at the energies involved was 0.3%.

The slit edges of the detector system were machined from nickel and hand lapped to a mirror surface. The slits were approximately 1 mm wide and 6 mm high, and their dimensions were measured with a Leitz split-image optical comparitor to ±0.001 mm, and the effective width and area were calculated from these measurements. The separation between slit holders was established by the use of polished blocks of known length and was determined to ±0.03 mm. The thickness of the slits is taken into account in the calculation of the G factor, along with making allowance for the fact that the horizontal and vertical defining rear slits were not coplanar, being separated by the thickness of one set of slits. The G factor was of the order of 1.2×10^{-5} cm.

Design of the slit and detector size was conservative to insure that there would be no possibility of loss of particles due to missing a slightly displaced detector or to multiple scattering in the first detectors. Except for considerations already mentioned, detector efficiency was deemed to be 100%. The count rate was insensitive to variation in detector voltage over a wide range of operating voltage, and runs measuring the same cross section were made over a period of many months and with different detectors and proved to be identical to within the 0.5% statistical accuracy of the test runs.

An additional shield and scraper slit was placed between the first collimating slit and the target foil to allow use of the detector system at small forward and backward angles. This shield prevented multiply-scattered particles from the portion of the target foil illuminated by the primary beam from being scattered by the first collimating slit and reaching the detectors. The inclusion of this slit shield greatly reduced the background seen at small angles without disturbing the detection of the desired particles.

F. Electronics and Computer

The output from each detector was fed to a charge-sensitive preamplifier with the output from each of the preamplifiers going into linear amplifiers having dual outputs to provide analog signals for energy information and pulses for consumption by coincidence circuitry. The analog signals were summed and ΔE and E signals were sent to analog-to-digital converters (ADC) for interfacing to an SDS 930 on-line computer. The computer calculated the mass of the detected particle according to the formula[16]

$$N_M = a\left[(E+\Delta E)^n - E^n\right],$$

where $N_M \propto M^{n-1}Z^2$ and a is a constant. In our experiment a value of $n=1.73$ was used. An arbitrarily set mass gate provided a mostly redundant coincidence to further eliminate background. In all cases very wide mass-gate limits were set to avoid possible losses. The signals entering the ADC's were gated by the coincidence circuit. Crossover timing was employed to time logic pulses for the coincidence circuitry, which had a resolution time of 1 μsec. Accidental coincidence rates, looked for with one pulse delayed, were so low that they were never observed with the counting rates used in this experiment.

An extensive effort was made to eliminate ground-loop problems between the various elements in the circuitry. Detailed studies of the effects of counting rates, timing jitter, pulse distortion, pileup, and dead times were made with the conclusion that the system could accurately handle, to the accuracy desired, 1000 detected particles/sec without unaccountably losing pulses. We normally limited the data rate to a conservative rate of 100 counts/sec and in all cases kept the rate less than 200 counts/sec. Twelve scalers with rate capacity of 50 MHz were utilized to monitor the various pulse functions and provide knowledge of possible pulse losses in the event of equipment malfunction. These scalers were interfaced to the computer for automatic data recording.

G. Faraday Cup and Charge Collection

A tantalum-backed water-cooled Faraday cup of large geometry was employed to measure the beam current. Leakage resistances for the cup were measured at the beginning of each experiment and in all cases were found to be in excess of 20 MΩ. The cup was equipped with devices to suppress electron currents, both electrostatic and magnetic for the secondary electrons emitted, and magnetic for delta rays ejected from the exit foil of the target. The delta rays may have 1000 times the energy of the secondary electrons and must be carefully suppressed.

The beam current was integrated and digitized

by a current integrator[17] incorporating a fast-response amplifier feedback to provide very low input impedance. The pulse output of the current integrator was recorded by a scaler and entered into the computer records.

III. EXPERIMENTAL PROCEDURE

A typical experiment proceeded as follows: After mechanically setting up and aligning the chamber, gains in the E and ΔE systems were equalized so that the sum signal properly represented the detected particle energy. Various electronic adjustments and tests were made and the acceptable mass limits were set on the computer, which permitted simultaneous acquisition of energy spectra for two independent sets of mass limits. The current integrator was calibrated and zeroed, and the calibration of the temperature and pressure sensing devices was established. With the aid of extensive check lists the proper functioning of various meters and scalers was determined, and the proper connection and continuity of various electrical connections was verified. The proton beam was steered and focused through the beam-optics system and the correct target position was verified by measuring beam transmission as a function of target angular position. A pulser spectrum which simulated the detected particle both in apparent mass and energy was made for future comparison in the event of suspected electronics difficulty, unusual noise levels, or gain changes. The target was filled and a gas sample was taken for later mass-spectroscopic analysis.

For each run at a given polar angle, the acceptance levels for the pulses entering the coincidence circuit were observed to assure that significant counts would not be cut from the tails of the various pulse-height distributions. Temperature and pressure were recorded at the beginning and end of each run so that an average target density could be calculated. In general, the variations in the pressure and temperature were small. When a sufficient number of counts were accumulated, two 800-channel spectra were printed, plotted, and written along with the other run parameters on magnetic tape for later computer analysis. A variety of functions were monitored during each run including detector bias, chamber pressure, beam optics, current-integrator zero, and operation of the electronics.

At each energy additional cross sections were measured at selected angles for D_2, C (as CH_4), N_2, and O (as CO_2) so that the fractional contamination of each of these components in the target could be determined from the original data and thus yield the purity of the principle target gas. It was found that greater accuracy in the determination of the target-gas purity could be made by analyzing the scattering spectra, although the mass-spectrographic analysis remained useful as an over-all check.

IV. ERRORS

The errors in a measured cross section will be discussed with reference to the formula

$$\sigma = (Y \sin\theta)/N_b N_T G ,$$

which gives the cross section in terms of the individually measured quantities. At the scattering angle θ, the yield Y is the number of elastically scattered particles, N_b is the number of beam particles traversing the scattering cell, N_T is the number of scattering centers per cm^3, and G, the well-known "geometry factor," contains the solid angle as defined by the detector collimating slits.[18] Known sources of systematic error which have been corrected for, as well as those which were found to have a negligible contribution, will be discussed. All errors quoted are standard deviations.

The error in the knowledge of N_T, the number of scattering centers per cm^3, came from several sources. The perfect-gas law was used to calculate the number of nuclei/cm^3. The error made in using the perfect-gas law as compared with using higher-order virial expansions with Van der Waals constants was less than 0.02% for the pressures and temperatures used in this experiment.

The pressure of the gas in the target cell was measured to ±0.2 Torr or about 0.1% of the normal operating pressure of 175 Torr. This included the effects of drifts in the electronics and uncertainty in the zero pressure reading. The limitation was due to the reproducibility of the pressure measuring instrument.

The error in the temperature measurement was ±0.2°C or 0.07% of the typical operating temperature of 298°K. This error includes the effects of beam heating on the target gas. An experimental verification of the negligible effects of beam heating was made by measuring a particular cross section at various beam currents from 120 to 400 nA. The results agreed to within 0.16%, which was the statistical uncertainty in the data. Calculations also indicated that beam-heating effects should be small (less than 10^{-4} deg). The response time of the thermocouple mounted on top of the target to temperature changes in the gas due to beam heating was calculated and found to have a time constant of less than a second. This effect was insignificant for our data runs which were always more than 5-min duration.

The purity of the target gas was measured for each target filling. With the gas filling system properly evacuated and the high-purity hydrogen used, the target gas was typically 99.7% pure. The impurities were determined by measuring the yield of protons elastically scattered from the heavier contaminants and comparing the effective cross section with previously measured cross sections for the contaminants such as oxygen and nitrogen. The error in the knowledge of the purity is typically 0.1–0.2%.

The resulting uncertainty in the calculated number of scattering centers was ±0.2–0.3%.

The integrated beam-current measurement was correct to ±0.2% down to an energy of 10 MeV and a detector angle of 10°. The current integrator itself was calibrated for each run with a precision current source (0.05%). The calibration stayed within ±0.1% over a period of a year. In order to be sure that the time constants of the integrator and switching errors did not affect the results, the data collection was started and stopped with a steady beam. An overscale cutoff device stopped the data accumulation if the beam current fluctuated above 95% of full scale.

Other considerations had to be made to insure that the desired accuracy was attained. The first consideration was whether the Faraday cup was collecting all of the beam that passed through the scattering cell. To insure that it was, the opening into the cup was designed to be six times the rms multiple-scattering angle for 10-MeV protons. An experimental verification that the Faraday cup was not missing scattered beam was made by doubling the target exit foil thickness and measuring a particular cross section for comparison with one previously measured with a single foil thickness. The two results agreed to ±0.5%, which was the statistical accuracy of the data. A further test was made to insure that the detector and slit assembly was not interfering with the beam collection at low detector angles by measuring a cross section with a monitor detector at 45° in the laboratory. Down to 10° there was no change in the cross section measured with the monitor detector to within ±0.4%, whigh again was the stastitical accuracy of the data. The effect of the chamber pressure on the beam collection was tested up to 10^{-5} Torr with no discernible effect. The chamber pressure during data acquisition was typically 5×10^{-7} Torr. Losses of the direct beam due to nuclear scattering in the target are less than 0.02%.

The G factor was calculated in the manner of Silverstein.[18] The error in the value of the G factor is ±0.2%. The primary limitation on the knowledge of the value is the accuracy with which the width of the slits can be measured (see Sec. II E). In addition, determination of exactly where the slits act added less than 0.1% uncertainty. Since the center of the turntable is not at the center of rotation, a small correction (0.4% at most), which depends on the detector angle, was made to compensate for this effect.

In calculating the G factor, only the first-order term was used; i.e.,

$$G = 2b_1A/R_0h\,,$$

where b_1 is the half-width of the front slit, A is the area of the rear slit, R_0 is the distance from the beam line to the rear slit, and h is the inter-slit distance. In the Silverstein calculations[18] there are higher-order terms which can have an important contribution in some cases. The maximum contribution for our apparatus from the first three correction terms is less than one part in 10^4. This includes the term due to the derivative of the cross section, which should be most important at forward angles (the contribution is 2 parts in 10^5 at 10° lab angle for 13.6-MeV $p+p$ scattering).

The effects of deviations from a line beam on the G factor were considered. The contributions due to a beam with a finite cross section but a parallel beam have been calculated by Silverstein. For our geometry this gave a correction of 5 parts in 10^5 maximum.

In the scattering cell the beam is not a parallel beam but has some divergence. This divergence depends on the beam optics and multiple scattering in the entrance foil and target gas. The magnitude of this effect has been calculated by Kan.[19] For the geometry used in this experiment, the magnitude of the correction is 0.15% at 10° in the laboratory and decreases rapidly with θ.

The accuracy with which the yield Y of elastically scattered protons is known is determined primarily by statistical uncertainties. The proton spectra at each angle were analyzed to subtract the background under the elastic peak due to slit-edge scattering and scattering from heavier contaminants. The background was typically 0.7% of the peak total with an estimated error in the background of 10% due to statistics and judgement. The background under the peak, due primarily to slit-edge penetration, was small because of the good energy resolution of the detector system. Once the background was subtracted, several other corrections were made to the yield. Dead-time corrections, mostly due to the ADC's, were on the order of 1%.

Data were taken at left and right angles and averaged to give the yield. This was done, since the included angle between two detector positions was known better (±0.02°) than the angle between

the beam center line and a single detector position (±0.06° maximum). This method also eliminates geometric errors due to any detector-system misalignment which may be present. The digital displays were readable to 0.01°. The final accuracy of the scattering angle including turntable position, beam direction, and slit position was ±0.03°.

In addition to these corrections, several other effects were considered and determined to contribute a negligible error (less than 0.1%). The detectors were assumed to have no dead areas. This was assured by making the detector slits small compared with the advertised active areas and by measuring a particular cross section repeatedly over a period of several months with different detectors and obtaining results consistent with no dead areas in the detectors.

Pileup effects were reduced by keeping the data rate to 100 counts/sec which was estimated to be a factor of 10 below the 0.5% loss rate. The effects of pileup, timing jitter, and other electronic distortions were tested with a random pulser, a double pulser, and different beam rates. Counts due to excited states of target contaminants were considered and determined to be negligible. For p-p scattering the elastically scattered protons from contaminants are separated by kinematic effects and correction did not have to be made for this even at the smallest angle.

There is a subtle question concerning the effects of multiple scattering of the scattered protons in the target exit foil. This multiple scattering could conceivably falsely increase or decrease the yield. However, it was found to have a negligible effect. The compensation by multiple scattering of protons in and out of the detector system was found to be essentially complete by a theoretical treatment.[20] We also experimentally verified complete compensation by measuring the p-T cross section at 160° where for 13.6-MeV incident protons, the scattered protons have an energy of approximately 3.5 MeV. The cross section was first measured with the standard target foil thickness and then with a doubly thick exit foil. The resulting cross sections were consistent within the statistics (0.4%). Thus, multiple scattering in the target exit foil was found to be self-compensating.

The largest error in the $\sin\theta$ term was 0.1% at the lowest angles.

Another source of error which was not included above was due to the uncertainty with which the scattering angle is known and the derivative of the cross section with angle. At 10° (the worst case) and with an angular uncertainty of 0.03°, this contribution to the error is 0.5%. At 12.5° the error contribution is down to 0.1%.

The central energy of the proton beams used was known to ±15 keV and has an energy spread of 20-keV FWHM, including the effects of foil and target-gas straggling and machine energy resolution. The beam was purified by magnetic analysis and, further, there was no experimental evidence of impurities in the beam.

In the previous discussion all errors contributing to the final value were discussed without regard to whether they contribute to the relative or scale error. The contributions to the scale error, i.e.,

TABLE I. Errors.

Scale		Relative	
Source	% Error	Source	% Error
Pressure	0.1	Yield	$1/\sqrt{N}$
Temperature	0.07	Background	~0.1
Purity	0.1–0.2	Dead time	0.0–0.06
G	0.2		
N_b	0.2		

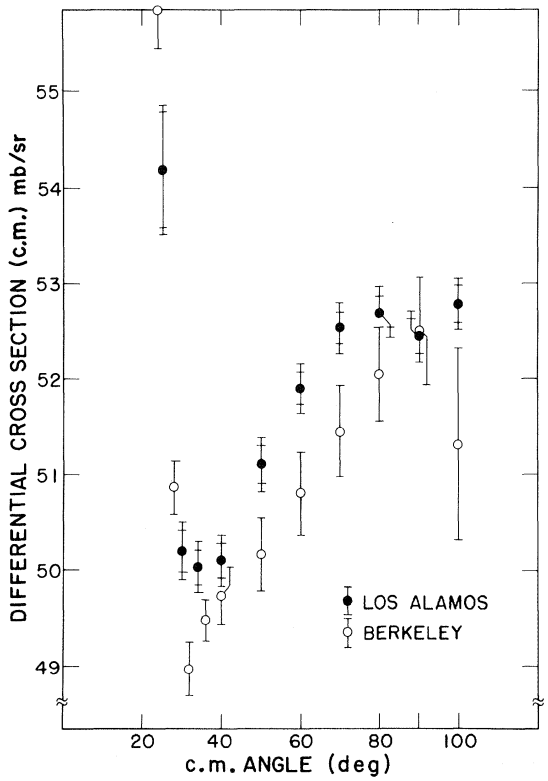

FIG. 2. Comparison of the Los Alamos and Berkeley (BGS) proton-proton elastic scattering data at 9.918-MeV lab bombarding energy. The errors shown for the Los Alamos data are the relative and absolute errors. Systematic absolute errors for the Berkeley data were reported to be negligible so that the error bars on their data indicate independent absolute errors (relative and absolute errors equal).

the normalization, include errors in N_T (due to pressure, temperature, and purity uncertainties), N_b, and G. Contributions to the relative error are primarily from the yield and the dead time. The relative and scale errors are combined to give the absolute error according to:

$$(\text{rel error})^2 + (\text{scale error})^2 = (\text{abs error})^2 .$$

Table I is a summary of the various sources of error which are not negligible.

V. DATA

The data are presented graphically in Figs. 2–4. In Fig. 4 the data of Kikuchi *et al.*[21] was multiplied by the ratio of the beam energies for comparison purposes. The measured cross sections are tabulated in Tables II and III. In the tables are listed the lab angle (known to ±0.03°) for each datum, the lab cross section in mb/sr, the equivalent c.m. angle and cross section along with the relative and absolute errors in standard deviations. The primary contribution to the relative errors is the statistics, with other sources of relative error contributing less than 0.2% in quadrature. The scale error for the 13.600-MeV data is 0.33% and is 0.37% for the other data. The beam energy was known to ±15 keV with a spread of 20-keV FWHM.

VI. DISCUSSION AND CONCLUSIONS

Comparisons with the Berkeley and Minnesota data are shown in Figs. 2 and 3. [We use[4] the Berkeley "BGS" data; see pp. 1124-1125 of Ref. 6.] The data may be compared with respect to both absolute normalization and shape. The Minnesota data at 9.69 MeV agree as well as can be seen by eye in both shape and normalization. There is a distinct disagreement between our data and the Berkeley data in normalization and some indication of a difference in shape. These observations are borne out in the calculations of Signell *et al.* in Refs. 4 and 8, and by our analysis in Ref. 10. Signell and Holdeman have analyzed[22] the 9.918-MeV data of Table II [omitting the 10° (lab) datum as it contributed an unusually high χ^2] and computed a value for ${}^1\delta_0^E$ of 55.23 ± 0.13° in good agreement with their prediction of Ref. 8. The value of

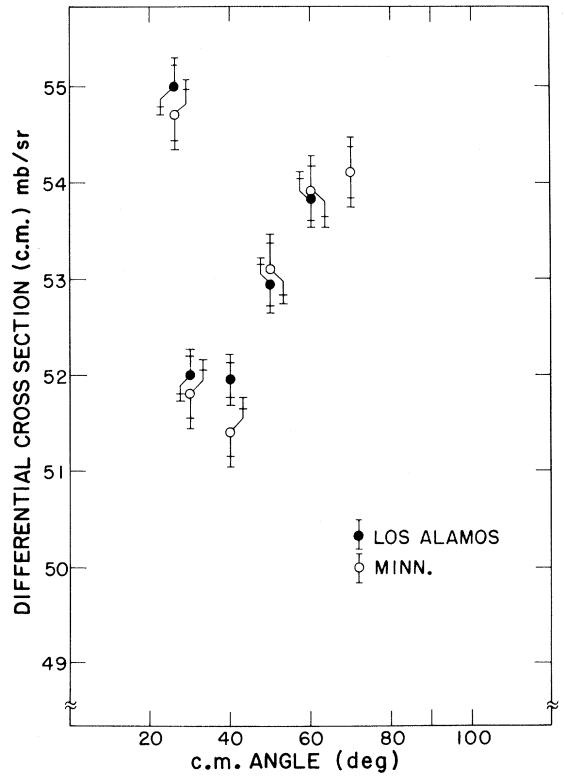

FIG. 3. Comparison of the Los Alamos and Minnesota proton-proton elastic scattering data at 9.690-MeV lab bombarding energy. The error bars indicate both the relative and absolute errors.

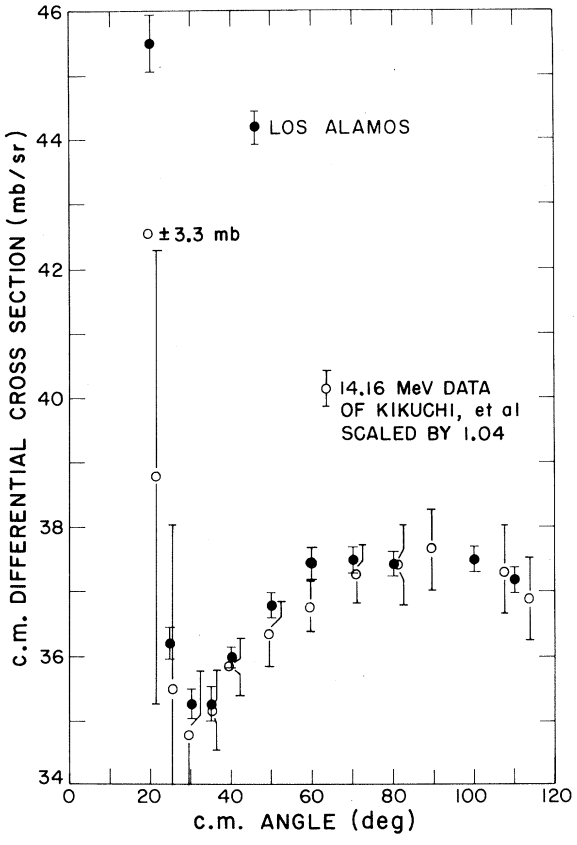

FIG. 4. Comparison of Los Alamos 13.6-MeV and Kikuchi *et al.* (see Ref. 21) 14.16-MeV proton-proton elastic scattering data. The data of Kikuchi *et al.* were scaled by the ratio of the energies (approximately 4%) to make the comparison. Their error bars are absolute.

TABLE II. Differential cross sections for $p+p$ elastic scattering.

θ_{lab} (deg)	$\sigma(\theta)_{lab}$ (mb/sr)	$\theta_{c.m.}$ (deg)	$\sigma(\theta)_{c.m.}$ (mb/sr)	Relative error (%)	Absolute error (%)
		9.918 MeV			
10.00	296.22	20.05	74.83	0.80	0.90
12.50	212.58	25.06	54.18	0.41	0.56
15.00	194.83	30.08	50.20	0.39	0.54
17.50	191.72	35.09	50.04	0.37	0.52
20.00	189.03	40.10	50.09	0.37	0.52
25.00	185.92	50.12	51.11	0.41	0.55
30.00	180.31	60.13	51.91	0.34	0.50
35.00	172.44	70.14	52.53	0.34	0.50
40.00	161.56	80.15	52.69	0.34	0.50
45.00	148.37	90.15	52.46	0.36	0.52
50.00	135.58	100.15	52.78	0.36	0.51
		9.690 MeV			
13.00	215.29	26.06	54.98	0.41	0.55
15.00	201.79	30.07	51.99	0.39	0.53
20.00	196.07	40.09	51.96	0.36	0.52
25.00	192.56	50.11	52.94	0.40	0.54
30.00	186.90	60.13	53.82	0.41	0.55

TABLE III. Differential cross sections for $p+p$ elastic scattering.

θ_{lab} (deg)	$\sigma(\theta)_{lab}$ (mb/sr)	$\theta_{c.m.}$ (deg)	$\sigma(\theta)_{c.m.}$ (mb/sr)	Relative error (%)	Absolute error (%)
		13.600 MeV			
10.00	180.44	20.07	45.50	0.94	1.00
12.50	141.88	25.09	36.09	0.57	0.66
15.00	137.18	30.10	35.28	0.51	0.61
17.50	135.37	35.12	35.28	0.58	0.67
20.00	136.02	40.13	35.99	0.31	0.45
25.00	134.00	50.16	36.79	0.35	0.48
30.00	130.12	60.18	37.43	0.51	0.61
35.00	123.15	70.19	37.49	0.35	0.48
40.00	115.29	80.20	37.58	0.36	0.48
50.00	96.24	100.20	37.48	0.38	0.50
55.00	85.15	110.19	37.20	0.38	0.51

$^3\Delta_c^E$, which is more sensitive to the shape of the angular distribution, was $-0.033 \pm 0.030°$. They calculate a χ^2 per point of 0.8 comparing our 9.918-MeV data with their prediction.

The $^1\delta_0^E$ point is shown in Fig. 5. The conflict between the phase shifts obtained from present data, the Minnesota data, the phenomenological prediction, and the phase shift derived from the Berkeley data is clearly evident. The situation with the P-wave parameter $^3\Delta_c^E$ is similar, as shown in Fig. 2 of Ref. 8.

In Fig. 4, we have taken the data of Kikuchi *et al.*[21] and multiplied their results by the ratio of the energies for a rough interpolation to compare with our 13.600-MeV data. The comparison by eye is

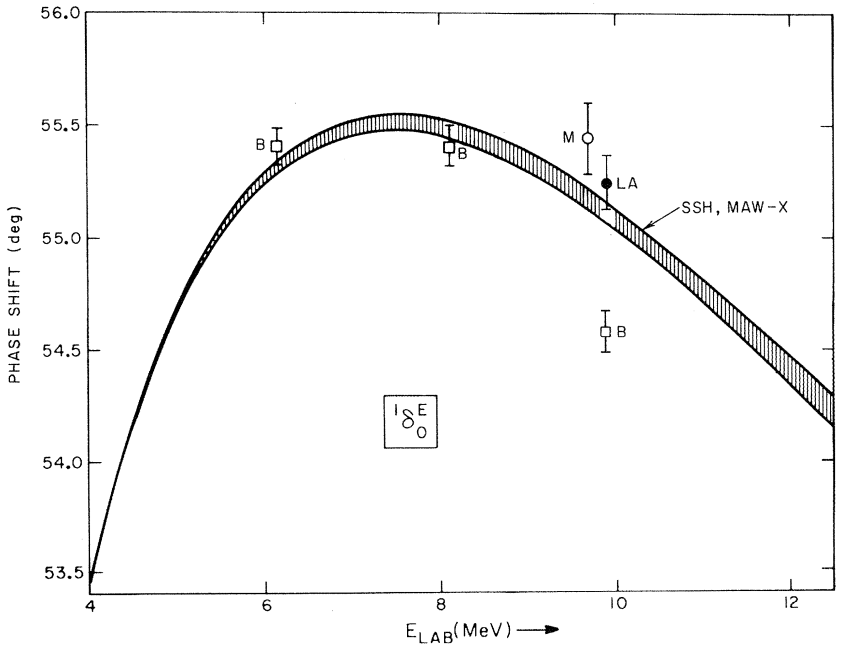

FIG. 5. Values of the $^1S_0$ electric-nuclear phase shift (see Ref. 4). The multienergy-analysis band is that of Refs. 2 and 4 (SSH), while the single-data-set error bars are from Refs. 4, 8, and 22. The data used in obtaining phase shifts are from Berkeley (see Ref. 6), Minnesota (see Ref. 5), and Los Alamos (see Ref. 10).

good in both normalization and shape. Further analysis of these data sets is in progress.[22]

Our over-all conclusion is that our $p+p$ scattering data in the region of 10 MeV now agrees with the detailed analysis of HSS[8]; and disagrees with the Berkeley data in both shape and absolute value. We anticipate that further analysis will continue to show that the present work has resolved the discrepancies in the phenomenological description of proton-proton scattering in the 10-MeV region.

ACKNOWLEDGMENTS

We are indebted to Ronald E. Brown for his extended help, advice, and support, and to Peter Signell, John C. Hopkins, and Leon Heller for useful discussions and suggestions. David Waymire also helped. The prosecution of the experiment would have been impossible without the continued cooperation and labors of the staff and operators of the accelerator facility, particularly Jules Levin and Martin Kellogg.

---

*Work performed under the auspices of the U. S. Atomic Energy Commission.

†Associated Western Universities Fellow, University of Wyoming.

[1]R. W. Stagat, F. Riewe, and A. E. S. Green, Phys. Rev. Letters 24, 631 (1970), and the references contained therein.

[2]M. H. MacGregor, R. A. Arndt, and R. M. Wright, Phys. Rev. 182, 1714 (1969) (MAW-X).

[3]R. E. Seamon, K. A. Friedman, G. Breit, R. D. Haracz, J. M. Holt, and A. Prakash, Phys. Rev. 165, 1579 (1968).

[4]M. S. Sher, P. Signell, and L. Heller (SSH), Ann. Phys. (N.Y.) 58, 1 (1970).

[5]L. H. Johnston and D. E. Young, Phys. Rev. 116, 989 (1959) ("Minnesota").

[6]R. J. Slobodrian, H. E. Conzett, E. Shield, and W. F. Tivol, Phys. Rev. 174, 1122 (1968) ("Berkeley").

[7]M. H. MacGregor, R. A. Arndt, and R. M. Wright, Phys. Rev. 179, 1624 (1969).

[8]J. Holdeman, P. Signell, and M. Sher, Phys. Rev. Letters 24, 243 (1970) (HSS).

[9]N. Jarmie, R. E. Brown, R. L. Hutson, and J. L. Detch, Jr., Phys. Rev. Letters 24, 240 (1970).

[10]N. Jarmie, J. H. Jett, J. L. Detch, Jr., and R. L. Hutson, Phys. Rev. Letters 25, 34 (1970).

[11]J. L. Detch, Jr., Ph.D. thesis, University of Wyoming, 1970 (unpublished).

[12]Hamilton Watch Company, Lancaster, Pennsylvania 17604.

[13]Equibar (TM), Trans-Sonics, Inc., Lexington, Massachusetts 02173.

[14]Wallace-Tienan, Inc., Belleville, New Jersey 07109.

[15]M. Q. Makino, C. N. Waddell, and R. M. Eisberg, Nucl Instr. Methods 60, 109 (1968).

[16]D. D. Armstrong, J. G. Beery, E. R. Flynn, W. S. Hall, P. W. Keaton, Jr., and M. P. Kellogg, Nucl. Instr. Methods 70, 69 (1969).

[17]Brookhaven Instruments Corporation, Brookhaven, New York 11973.

[18]E. A. Silverstein, Nucl. Instr. Methods 4, 53 (1959).

[19]T. C. Kan, M.S. thesis, University of Minnesota, 1969 (unpublished).

[20]J. H. Jett, J. L. Detch, Jr., and N. Jarmie, to be published.

[21]S. Kikuchi, J. Sanada, S. Suwa, I. Hayashi, K. Nisimura, and K. Fukunaga, J. Phys. Soc. Japan 15, 9 (1960).

[22]P. Signell, Michigan State University, private communication.